The ANTICS Large-N Seismic Deployment in Albania

Hans Agurto-Detzel[1*], Andreas Rietbrock[1], Frederik Tilmann[2,3], Edmond Dushi[4], Michael Frietsch[1], Ben Heit[2], Sofia-Katerina Kufner[1,5], Mike Lindner[1], Besian Rama[4], Bernd Schurr[2], Xiaohui Yuan[2].

[1] Karlsruhe Institute of Technology, Geophysical Institute, Germany.
[2] Deutsches GeoForschungsZentrum (GFZ), Potsdam, Germany.
[3] Freie Universität Berlin, Germany.
[4] Department of Seismology, Institute of Geosciences, Polytechnic University of Tirana, Albania
[5] Now at GeoZentrum Nordbayern, Friedrich-Alexander University Erlangen-Nürnberg, Germany
[*] Corresponding author: hans.detzel@kit.edu

October 15, 2024

The ANTICS Large-N Seismic Deployment in Albania

Hans Agurto-Detzel[1*], Andreas Rietbrock[1], Frederik Tilmann[2,3], Edmond Dushi[4], Michael Frietsch[1], Ben Heit[2], Sofia-Katerina Kufner[1,5], Mike Lindner[1], Besian Rama[4], Bernd Schurr[2], Xiaohui Yuan[2].

[1] Karlsruhe Institute of Technology, Geophysical Institute, Germany.
[2] Deutsches GeoForschungsZentrum (GFZ), Potsdam, Germany.
[3] Freie Universität Berlin, Germany.
[4] Department of Seismology, Institute of Geosciences, Polytechnic University of Tirana, Albania
[5] Now at GeoZentrum Nordbayern, Friedrich-Alexander University Erlangen-Nürnberg, Germany
[*] Corresponding author: hans.detzel@kit.edu

Abstract

Located within the active continental collision between Eurasia and the Adriatic microplate, Albania is an earthquake prone country with one of the highest seismic risk in Europe. This came into evidence when the M_W=6.4 Durrës earthquake hit the country in 2019, causing 51 fatalities and widespread damage to infrastructure. Despite this stark reminder, the seismotectonics of Albania remain poorly researched, holding many unknowns regarding active seismogenic faults and 3D velocity structure. In an attempt to fill-in this knowledge gap, we conceived the project ANTICS (AlbaniaN TectonIcs of Continental Subduction) to install a temporary arrangement of 382 seismic stations, and densely monitor the abundant seismic activity in central Albania. In this paper we introduce the project goals and seismic deployment, assessing data quality and extracting valuable lessons from such a complex large-N deployment. Finally, we present some preliminary results on the detected seismicity and a receiver function profile, and expand on the outlook of the project and possible next steps in the area.

Introduction

Albania sits at the southwestern part of the actively convergent boundary between the Eurasian plate and the Adriatic microplate (Fig. 1). As such, compressive tectonics with active shortening in the SW-NE direction and NW-striking thrusts and folds dominate, particularly in the coastal areas. Tectonically, the country is dominated by the presence of the Albanides, the middle section of the Dinarides-Hellenides fold-and-thrust belt that was formed east of the Adriatic Sea since the Late Jurassic as part of the large-scale convergence between Eurasia and Africa. The regional seismotectonics is thus controlled by the

aforementioned system of NW-SE thrust faulting, but also by two major NE-SW strike-slip structures that control the sedimentary emplacement and tectonic evolution of the Albanides. These tectonic lineaments are the Shkodër-Peja Fault to the north, which separates the Albanides from the Dinarides, and the Vlorë-Elbasan lineament in the south.

The Albanides orogen is divided into two domains: (1) the Internal or Eastern Albanides, composed by metamorphic sequences, and (2) the External or Western Albanides, characterized by Triassic to Eocene carbonates and Oligocene to Pliocene siliciclastic deposits. The Albanides division also reflects into the deformation style: while the External Albanides and foredeep are still undergoing shortening with active SW-verging folding and thrusting, the Internal Albanides are currently undergoing extension and uplift (Vittori et al., 2021 and references therein).

In our study region, the Moho depth increases from 25-30 km under the Adriatic Sea to 40-50 km under the Albanides axis, whilst the maximum seismogenic depth tends to follow the Moho, with hypocenters mostly in the upper crust down to 20 km depth (Stipcevic et al., 2020). Small earthquakes (M<4.5) are ubiquitous in Albania, with an M4.5+ earthquake every 1.3 years on average (Aliaj et al., 2010; Muço et al., 2013). Most larger earthquakes (M>5) occur along three well recognized seismic belts: (1) the NW-trending Ionian-Adriatic coastal thrust belt, (2) the N-S trending Peshkopia-Korçë graben fault zone at the East of the country, and (3) the transversal NE-trending Elbasani-Dibra-Tetova normal fault belt that crosses the previous two (Aliaj et al., 2004). Records of historical seismicity show 55 earthquakes with intensity (MSK) larger than VIII up until the 20th century (Aliaj et al., 2010). During the instrumental era (~1900 onwards), 418 events with M>4.5 occurred up until the year 2000 (Sulstarova et al., 2001). Based on the historical records, Aliaj et al. (2004) estimated the maximum earthquake magnitude for the Albanian territory to be 7.25.

Recently, in November 2019, an M_W 6.4 earthquake struck the port town of Durrës with a rupture on a NNW-trending shallowly dipping thrust fault at a depth of 22 km (Teloni et al., 2021). The complete sequence included two M>5 foreshocks and thousands of aftershocks lasting at least throughout January 2020 (Teloni et al., 2021, Van der Heiden, 2022). The occurrence of this important earthquake and the lack of studies regarding the seismogenesis and velocity structure of the Albanian territory, prompted the conception of the project ANTICS (AlbaNian TectonIcs of Continental Subduction).

The ANTICS deployment

The large-N ANTICS deployment is an international collaborative effort led by the Karlsruhe Institute of Technology (KIT, Germany), the German Research Center for Geosciences (GFZ, Germany), and the Institute of GeoSciences, Energy, Water and Environment of the Polytechnic University Tirana (PUT, Albania), that builds up on our previous Durrës aftershock deployment in the region (Schurr et al., 2020). The goal of the ANTICS project is to explore in detail the seismogenic sources and velocity structure within the Albanian territory, filling in the gap of knowledge persistent in this region. Among the expected results, we aim to obtain an accurate local earthquake catalogue and a detailed crustal structure from local earthquake tomography, full waveform tomography, ambient noise tomography and receiver function analysis.

The initial network deployment (Phase 1) was carried out by five teams of two people each, during a 3-week period between September 23 and October 13, 2022 (Fig. 1). All instruments were obtained from the GFZ and KIT seismic pools, with a total of 382 stations installed, including 50 broadband seismometers (Trillium Compacts with flat response up to 120 s) and 332 3-component geophones (PE-6B with 4.5 Hz corner frequency) recording at a sampling rate of 100 Hz. The average inter-station spacing was 6 km, with a total covered area of 130×145 km^2, encompassing a large part of the Albanian territory including its full W-E extension. The elevation of station sites varied from sea level to 1740 m, with an average of 533 m.

During servicing in May 2023, the network geometry was reconfigured into four lines for a receiver function experiment (Phase 2; Fig. 2a). Three lines were deployed perpendicular to the orogeny, while the fourth one was deployed along strike. The nominal inter-station spacing within the lines was 1 km, and because of logistical constraints, the installation occurred mostly along roads. A total of 214 geophone stations were moved to these new sites, while the rest of the original sites, including all 50 broadband stations, were left in place as a backbone areal distribution. This new configuration remained in place until March 2024, when all stations were permanently removed.

The temporary setup for each site consisted of a sensor buried at ~50 cm depth, and in a separate hole the data logger, GPS antenna, battery and cables, semi-buried and covered by an inverted plastic bucket (Fig. 3). Sensors were oriented according to magnetic north; the

magnetic declination in the study region during the deployment period was 5°. DATA-CUBE 3-channel recorders were used for all stations, with a gain set at 1 for broadband sensors and 16 for short period sensors. The power source consisted of one (two for broadband stations) non-rechargeable 9v/175Ah dry alkaline battery, providing an estimated autonomy of ~9 months. Importantly, because the alkaline batteries were of type metal-air, they had to have access to fresh air and therefore we kept them in a non-waterproof setup allowing proper ventilation but potentially also allowing the access of water and insects. For stations at elevations above 1000 m where freezing temperatures were expected in winter, we opted for using sealed battery packs of lithium batteries.

The most important challenges faced during installation were related to excess of rain and flooding on the roads, unreliable GPS navigation in remote areas, and mechanical car problems mostly due to the generally poor road infrastructure. Because of the high density deployment, some of the stations (47) had to be installed outside properties in open conditions, though all broadband sensors were installed within properties for safety reasons. During the second phase, and due to the denser and more strict location of the profiles stations, a total of 110 out of the 214 stations had to be installed outside properties.

Data quality and recovery

Servicing of the entire network was carried out in mid-May 2023. Average data recovery was 76% (median=93%), with 287 (75%) stations recording for 50% of the time or more (Fig. 4). Five stations were unfortunately stolen and therefore not possible to recover.

The most common cause for incomplete data recovery was battery failure due to flooding. In fact, the average last day recorded for flooded stations was 18 December 2022, which is right after the peak of the rainy season in Albania (Fig. 5). In contrast, the average last recorded day for all stations is 20 March 2023. In total 43 (11%) sites were found with clear signs of flooding, although this is a lower bound, given that flooding signs were not always visible or this information was not always collected. Notably, all the flooded sites, except for one, were installed inside a farm or backyard, mostly in clay-rich soils for a lack of a better location. Furthermore, while the average elevation for all stations was 533 m, the average elevation for flooded stations was only 294 m, which again indicates that farming soils at lower elevations had a tendency to flooding, while at higher elevations, rocky soils with better permeability were better suited for our installation. Overall, the data suggest that once a given station

survived the rainy period, chances are that it recorded until the servicing in May or shortly before that. Furthermore, no battery problems were observed due to low temperatures at high altitude.

Fig. 6 shows the noise levels for all broadband and short-period stations during the first phase (September 2022 to May 2023) as Probabilistic Power Spectral Density (PPSD) median curves of their vertical component (e.g. Custodio et al., 2014). In general, broadband stations noise levels are below the high noise model, except for five stations that show higher noise levels at periods between 0.2 and 2 s. Geophones show a similar distribution, with higher noise levels between 02-2 s, and instrumental self-noise dominating for periods longer than about 5 s. The secondary microseismic noise peak occurs at 2-3 s, at significantly shorter period than the global average. In general, stations installed outside properties are considerably quieter than stations inside properties (Sup. Fig. 1), but a few free-field stations installed outside properties still present high levels of noise.

Similarly, Fig. 7 shows PPSD median curves for the short-period stations included in the four RF lines during the second phase (May 2023 to March 2024). In general, line-500 seems to be the quieter one, with the other three lines showing a more diverse range of noise amplitudes, some of them above the high noise model. Notably, line-500 was deployed in the more remote and mountainous southern area, while the other 3 lines, particularly lines 600 and 800, were deployed along important roads with nearby populated centres. This can be better seen in Fig. 8, which shows in map view the average median noise amplitude for all stations in the period range 0.05 to 2 seconds. There appears to be a clear trend from northwestern noisier stations to southeastern quieter stations. This can be explained as the NW contain low elevation lands close to the sea, with nearby important populated centres. On the other hand, as we move to the SE we gain in elevation, depart from the sea and the population is more scarcely distributed. A clear exemption to this rule are the somehow noisier stations located nearby Korçë, which can be justified precisely by the presence of this city, the largest in eastern Albania. On a closer examination, a more direct first order anti-correlation seems to exist between noise amplitude and terrain slope. For example, the middle section of the line-700 contains anomalously noisier stations in a flatter valley area in comparison with the surrounding stations in areas of greater slope. This also holds true for the noisier stations north of Korçë. Certainly flatter areas are more populated and bisected by more transited roads as opposite to roughed terrain where more scarce population is expected

and therefore lower anthropogenic noise levels. Also, flatter areas are generally covered by a thicker sedimentary layer that amplifies the seismic noise, whilst rougher terrain often correlates with the outcrop of more compact rocks. In fact, the distribution of noisier stations (orange and red colours) matches very wall that of the Neogene-Quaternary deposits (e.g. Teloni et al., 2021). Still, it could be interesting for future deployments to consider an easily available parameter such as elevation or terrain slope as a first order indication of expected noise level (Sup. Fig. 2), in addition to other more obvious but harder to obtain parameters such as population density, road traffic or geology.

Preliminary Earthquake Catalogue

The continuous waveforms collected from September 2022 to May 2023 were processed with an AI-based automatic picker PhaseNet (Zhu et al., 2019), obtaining 38.4 M picks of which 20.8 M are P phases and 16.6 M are S phases. These picks were then associated into events using the AI-based HEX algorithm (Woollam et al., 2020, 2022). For this step we used a selection of 95 homogenously distributed stations given that the use of all 382 densely placed stations produced an excess of false detections. Nearly 18k events were detected with at least 8 P- and 3 S-phases, associating 1.93 M picks. All 18k events were then relocated using a 1-D velocity model (Dushi and Havskov, 2023) and the NonLinLoc algorithm (Lomax, 2009) which provides a full probabilistic density function for each hypocentral location.

Local magnitudes were calculated using maximum peak-to-peak amplitudes of the S-phase on the horizontal components and an empirical relationship for the region (Muço and Minga, 1991). We then benchmarked and corrected our estimations with 1028 common events from the manually picked local earthquake catalogue of the IGEO-PUT (Bulletin of the Albanian Seismic Network), obtaining a simple linear trend with a slope of nearly 1 but a positive bias of 0.4 magnitude units with respect to the local catalogue (Fig 9). After correcting for this bias, our final magnitudes range from -1.0 to 4.5, with a magnitude of completeness (Mc) of ~1.5. Five earthquakes M_L>=4.0 occurred during the deployment period, the largest of them associated to the January 2023 Klos sequence.

The temporal evolution of seismicity (Fig. 10) shows an average daily rate of 70 earthquakes per day, while two maxima of 700-800 events per day are observed associated to the Klos and Erseke sequences, respectively. Figure 11 shows a selection of ~10800 events with at

least 10 P, 4 S, and location uncertainties less than 5 km. The seismicity seems to be distributed in clusters and along known major structures. Events occur down to 30 km depth, notably with a decrease of the seismogenic depth from 30 to 20 km depth from North to South. Noteworthy is the fact that no seismicity is observed in the epicentral area of the 2016 Durrës earthquake, which would indicate a complete return to background seismicity levels following the aftershock period of that earthquake (Van der Heiden, 2021).

Two earthquake clusters were particularly productive during our study period: to the north, the Klos sequence occurred in January 2023, and to the south, the Erseke sequence, occurred in March 2023. The Klos sequence seems to start on the January 13 with an M_L 3.0 earthquake, which elevates the daily rate of seismicity to nearly 400 events per day in the nearby area (Sup. Fig. 4). The following next two days the seismicity rate decays until the evening of the 15 of January when the M_L 4.5 mainshock occurs, which again elevates the daily rate of seismicity to above 700 events per day. The whole sequence is confined to depths 5-20 km depth, with all hypocenters M_L>=3.0 near the bottom of the seismogenic layer, ranging 15-20 km depth. Spatially, the seismicity seems to be associated to a large normal fault NW-striking. This is corroborated by our moment tensor solution for the Klos mainshock, which indicates oblique normal faulting with a similar strike (Fig. 11).

The Erseke sequence started with an M_L 4.3 mainshock on the 23 of March 2023, which elevated the daily rate of seismicity to almost 800 events per day in the nearby area. For the next ten days, the seismicity rate decays, although some bursts of seismicity are seen on the March 24 and 26 as secondary aftershock sequences of large aftershocks (Sup Fig. 5). The seismicity occurs mostly between 3 to 17 km depth, with the mainshock hypocenter located at 17 km. Spatially, the sequence is associated to a large oblique normal fault striking NNE (Fig. 11).

Preliminary receiver function analysis

Passive-source seismic imaging using the receiver function (RF) method is commonly used to study the structure in the crust and upper mantle. Conventional RFs are computed using broadband data and are usually stacked over a large number of teleseismic events to enhance the signal/noise ratio. In recent years the use of short-period stations has been greatly increased and has proven successful in extracting RFs (Yuan et al. 1997; Ward et al. 2017). Here we show that it is feasible to apply the RF analysis to the ANTICS Large-N experiment.

Fig. 11 is a preliminary Common-Conversion-Point (CCP) stacked RF cross section along one of the linear profiles with densely spaced stations (Line-600). Ten events with magnitudes greater than 6.5 occurring between October 2022 and July 2023 are used, five in the first phase and five in the second phase of the experiment (Fig. 11a). The majority of the stations are short-period Geophones with a natural frequency of 4.5 Hz, which is outside the normal teleseismic frequency range usually of 0.1-1 Hz. Therefore, the instrument response has been deconvolved from the raw data to enhance the teleseismic signals and simulate broadband records. Three-component data are visually inspected and processed with the RF analysis, which mainly involves component rotation and deconvolution. RF cross sections were constructed along the four linear profiles with a swath width of 20 km. Figure 11c is an example of Line-600, along with some conspicuous crustal interfaces. The profile crosses a prominent sedimentary basin to the west and a mountainous area to the east. The interface at shallow depths down to 20 km may represent the crystalline basement that dips to the west. The exact depth requires further correction with the seismic velocity of the sediment. The multiples of the basement may dominate the 40-60 km depth range. There appears to be evidence of the Adriatic Moho that dips to the east to a depth of 65 km. Further analysis with the complete dataset is needed to verify these preliminary observations.

Lessons learned and outlook

Given the density and large number of installed stations, and despite the adverse road and meteorological conditions, the ANTICS deployment was swiftly and successfully achieved. In a period of three weeks during September-October 2022, we managed to install 382 seismic stations in a wide range of terrain and elevation conditions. Considering the installation and subsequent servicing, we gathered the following valuable lessons:

(a) More attention to meteorological and seasonal conditions should be taken into account for the deployment schedule to reduce the likelihood of data loss due to intense rain periods. In that sense, when a rainy period lies within the deployment period, a service run checking on the stations should be organised as soon as possible thereafter.

(b) It is important to consider the soil permeability of the sites, in order to avoid flooding due to poor permeability. A good rule of thumb is to avoid clay-rich farming soils.

(c) Metal-air batteries are a good option for temporary deployments such as ours, but attention should be put into not burying too much the batteries and always keeping the

upper half of it above surface to avoid penetration and accumulation of water. This of course has to be balanced with the fact that the equipment should be concealed to avoid robbery and damage when installing outside properties.

(d) Once a station continued working during the rainy season, chance is that it will record until the end. In that sense, there were no problems inherent to battery durability, at least during the first phase of our experiment.

(e) Having said that, we did experience some battery problems during the second phase, likely due to a bad batch of batteries with reduced capacity due to extended time in storage. Therefore, checking the batteries capacity before installation is recommended.

Data availability

The ANTICS dataset (network code X3; https://geofon.gfz-potsdam.de/waveform/archive/network.php?ncode=X3&year=2022) will be openly available at the GEOFON web service from May 2028.

Acknowledgments

We are indebted to all the Albanian landowners that allowed us to install stations in their properties and looked after them during the project. We also thank all the personnel involved in the installation and servicing of stations, and related logistics: Felix Bögelspacher, Benedikt Braszus, Arnaud Dalsuc, Marson Dyrmishi, Susanne Hemmleb, Rune Helk, Laura Hillmann, Damiano Koxhaj, Agur Lybeshari, Peter Makus, Lenny Mejía, Leon Merkel, Dionald Muçollari, Christoph Sens-Schönfelder, Gjergji Stoja, Indrit Rexhepi, Susann Richter, Gjon Rota, Thomas Zieke, Arben, Rrezart, Olgert, Gazmir, Klei, Marcel.

References

Aliaj, Sh., Adams, J., Halchuk, S., Sulstaorva, E., Peci, V., Muço, B. 2004. Probabilistic hazard maps for Albania. 13th WCEE Vancouver, Canada, August 1-6, 2004, Paper No 2469.

Aliaj, S., Kociu, S., Muço, B. & Sulstarova, E., 2010. Seismicity, Seismotectonics and Seismic Hazard Assessment in Albania, Academy of Sciences of Albania, pp. 98.

Bulletin of the Albanian Seismic Network. Monthly bulletin of seismology. Country: Albania. Medium: Online, ISSN:2664-410X. https://www.geo.edu.al/Services/Department_of_Seismology/

Custódio, S., Dias, N.A., Caldeira, B., Carrilho, F., Carvalho, S., Corela, C., Díaz, J., Narciso, J., Madureira, G., Matias, L. and Haberland, C., 2014. Ambient noise recorded by a dense

broadband seismic deployment in western Iberia. Bulletin of the Seismological Society of America, 104(6), pp.2985-3007.
Dushi, E.D. and Havskov, J., 2023. 1D crustal structure of Albania region. Annals of Geophysics, 66(1), pp.SE103-SE103.
Lomax, A., Virieux, J., Volant, P. and Berge-Thierry, C., 2000. Probabilistic earthquake location in 3D and layered models: Introduction of a Metropolis-Gibbs method and comparison with linear locations. Advances in seismic event location, pp.101-134.
Muço, B.,2013. Probabilistic seismic hazard assessment in Albania. Italian Journal of Geosciences 132(2): 194–202. https://doi.org/10.3301/ijg.2012.33.
Schurr, B., Dushi, E., Rietbrock, A., Duni, L. 2020. AlbACa Albanian Earthquake Aftershock Campaign. GFZ Data Services. Other/Seismic Network. doi:10.14470/4X7564679396.
Stipčević, J., Herak, M., Molinari, I., Dasović, I., Tkalčić, H. and Gosar, A., 2020. Crustal thickness beneath the Dinarides and surrounding areas from receiver functions. Tectonics, 39(3), p.e2019TC005872.
Sulstarova, E., Aliaj, Sh. 2001. Seismic Hazard Assessment in Albania. Albania Journal Of Natural & Technical Sciences 10: 89-100.
Teloni, S., Invernizzi, C., Mazzoli, S., Pierantoni, P.P. and Spina, V., 2021. Seismogenic fault system of the Mw 6.4 November 2019 Albania earthquake: New insights into the structural architecture and active tectonic setting of the outer Albanides. Journal of the Geological Society, 178(2), pp.jgs2020-193.
Van der Heiden, V. 2021. Analysis of the 2019 Mw 6.4 Albania aftershock sequence: An updated velocity model using AI-based solutions, Master's thesis, Karlsruhe Institute of Technology, Geophysical Institute.
Vittori, E., Blumetti, A.M., Comerci, V., Di Manna, P., Piccardi, L., Gega, D. and Hoxha, I., 2021. Geological effects and tectonic environment of the 26 November 2019, M w 6.4 Durres earthquake (Albania). Geophysical Journal International, 225(2), pp.1174-1191.
Ward, K. M., & Lin, F. C., 2017. On the viability of using autonomous three-component nodal geophones to calculate teleseismic Ps receiver functions with an application to Old Faithful, Yellowstone. Seismological Research Letters, 88(5), 1268-1278.
Woollam, J., Rietbrock, A., Leitloff, J. and Hinz, S., 2020. Hex: Hyperbolic event extractor, a seismic phase associator for highly active seismic regions. Seismological Society of America, 91(5), pp.2769-2778.
Woollam, J., Münchmeyer, J., Tilmann, F., Rietbrock, A., Lange, D., Bornstein, T., Diehl, T., Giunchi, C., Haslinger, F., Jozinović, D. and Michelini, A., 2022a. SeisBench—A toolbox for machine learning in seismology. Seismological Society of America, 93(3), pp.1695-1709.
Yuan, X., J. Ni, R. Kind, J. Mechie, and E. Sandvol., 1997. Lithospheric and upper mantle structure of southern Tibet from a seismological passive source experiment, J. Geophys. Res. 102, no. B12, 27,491–27,500.
Zhu, W. and Beroza, G.C., 2019. PhaseNet: a deep-neural-network-based seismic arrival-time picking method. Geophysical Journal International, 216(1), pp.261-273.

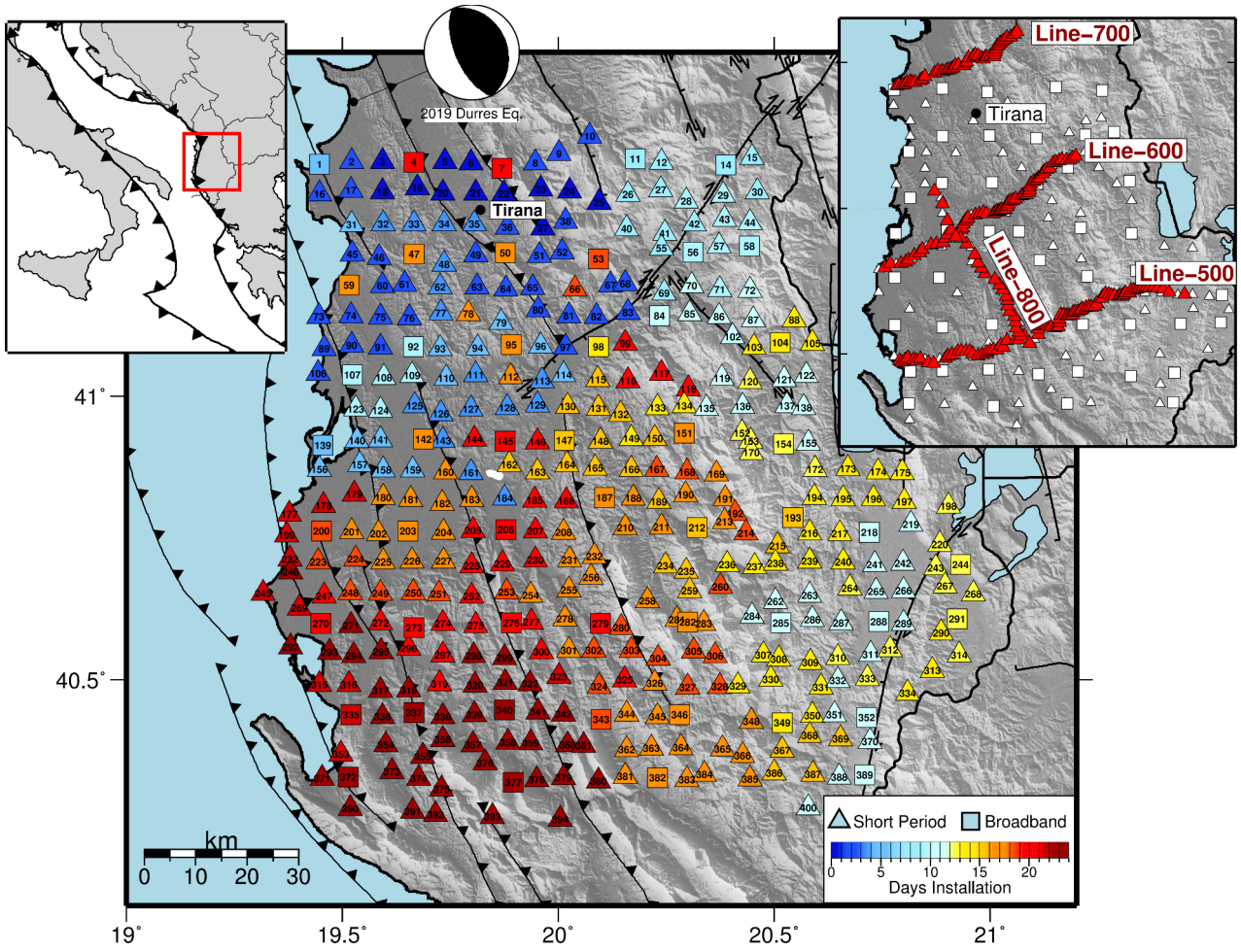

Figure 1. Location and first phase network deployment coloured by installation date. Focal mechanism of 2019 Mw=6.4 Durrës earthquake, taken from USGS moment tensor solution. Top-right inset: receiver function lines and areal stations remaining throughout the second phase.

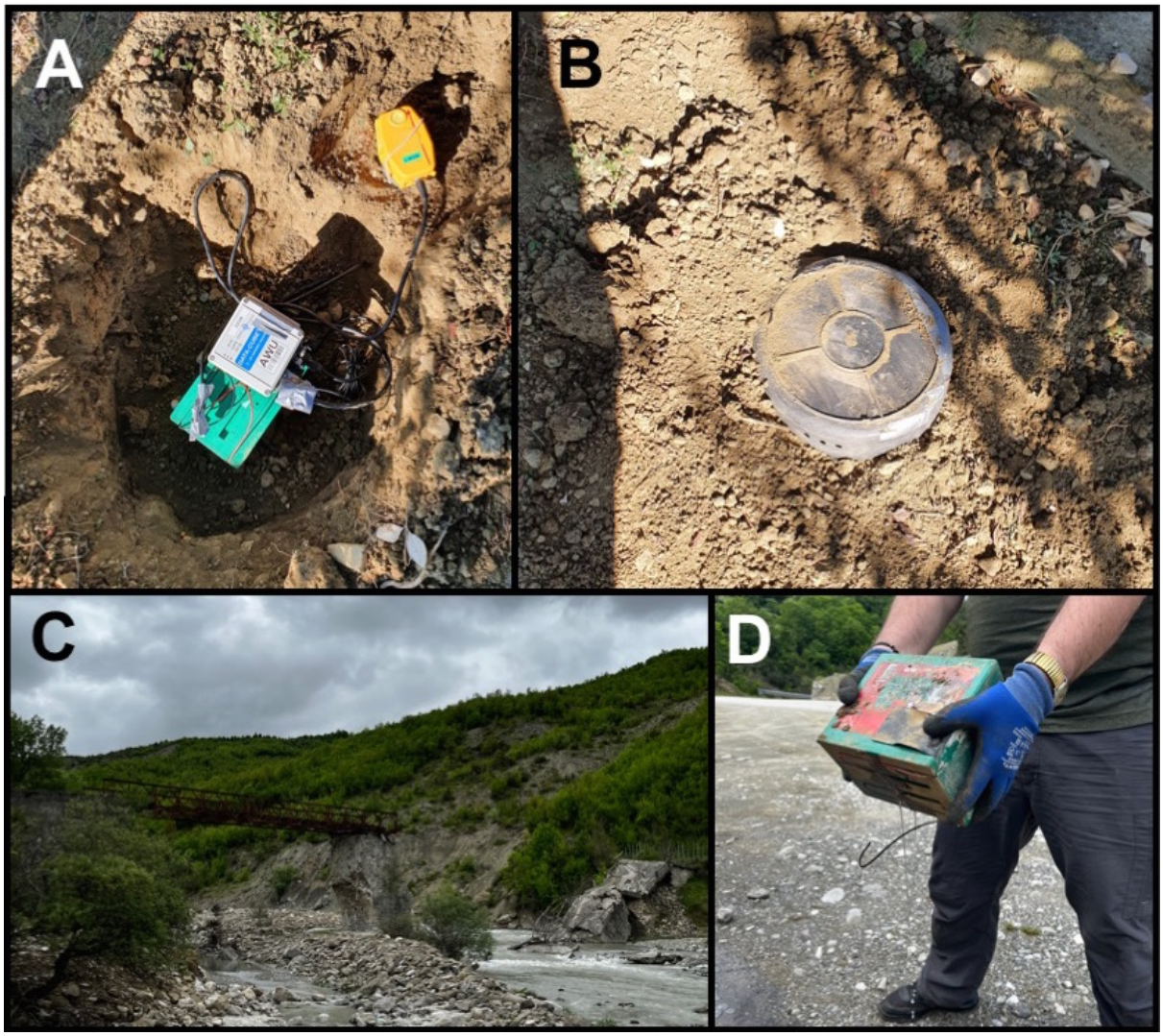

Figure 2. Composite of photos showing setup and deployment. A: initial setup with geophone, battery and Cube recorder. B: the sensor is buried and covered by soil, and the recorder and battery are covered by an inverted plastic bucket with small holes on the sides to allow for ventilation. C: Some of the difficulties during fieldwork included flooded paths and broken road infrastructure. D: flooded battery found during servicing in May 2023.

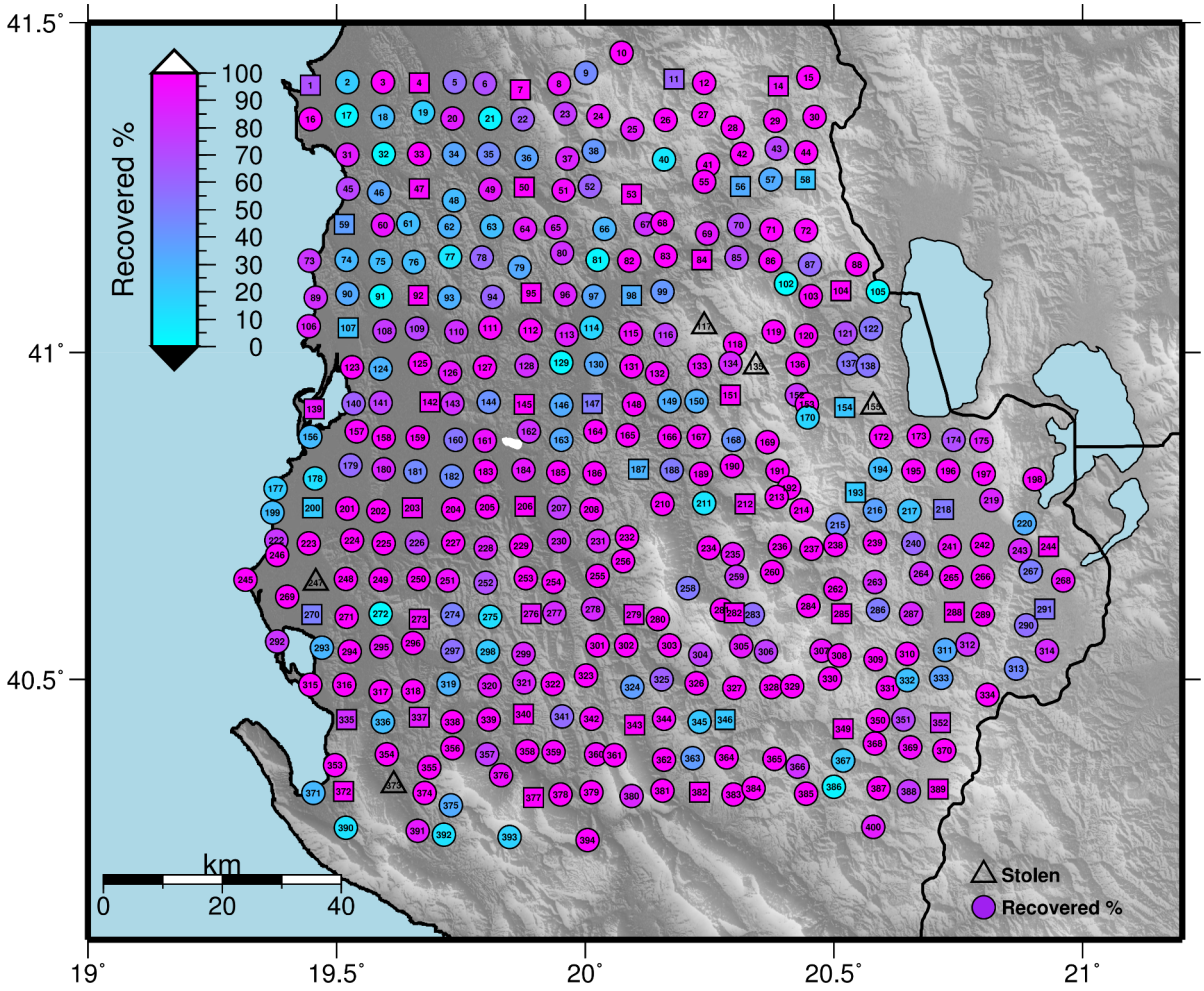

Figure 3. Data recovery during first service, May 2023.

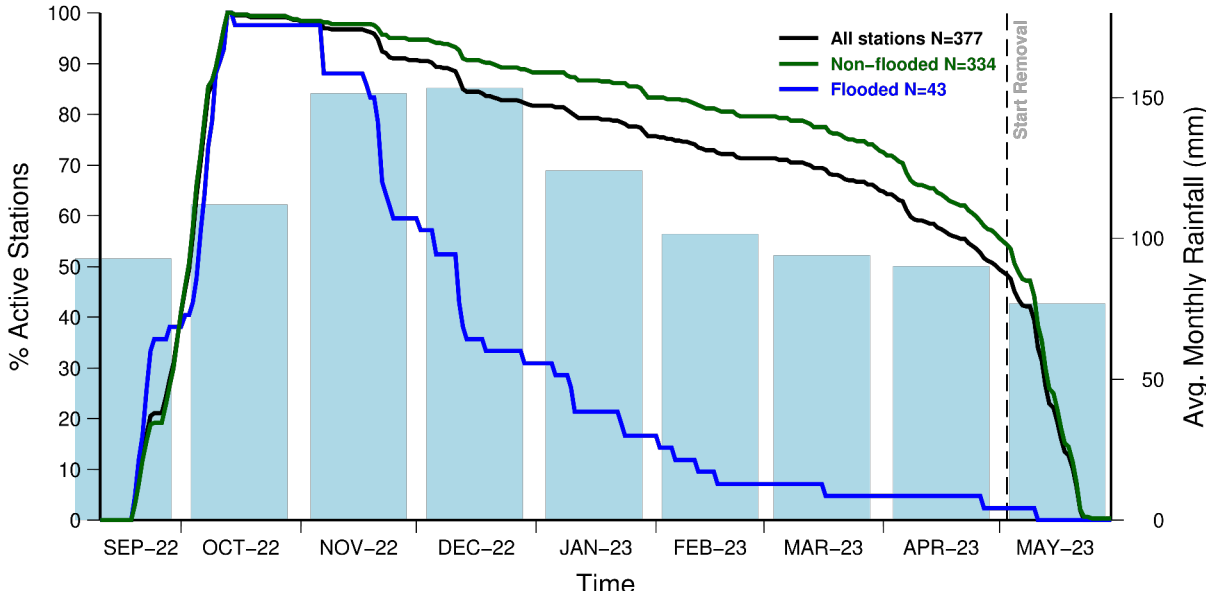

Figure 4. Correlation between active stations and historical rainfall as a function of time. Steep fall in active stations coincides with periods of heavy rainfall and therefore potential site flooding. Precipitation data from https://climateknowledgeportal.worldbank.org/country/albania/climate-data-historical (last visited 12 October 2024).

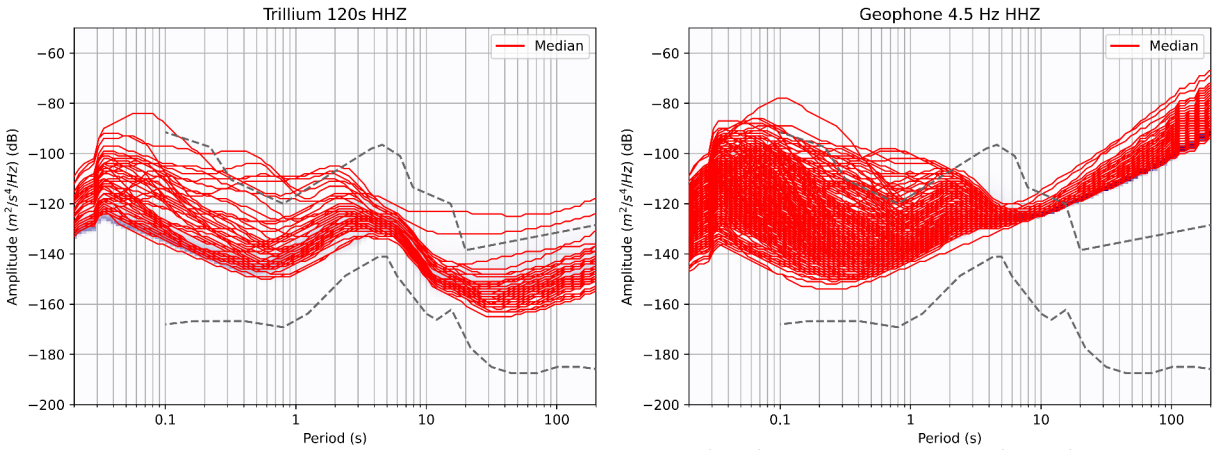

Figure 5. PPSD curves of noise median for broadband (left) and short period (right) stations, corresponding to the first phase of the project (Septermber 2022 – May 2023).

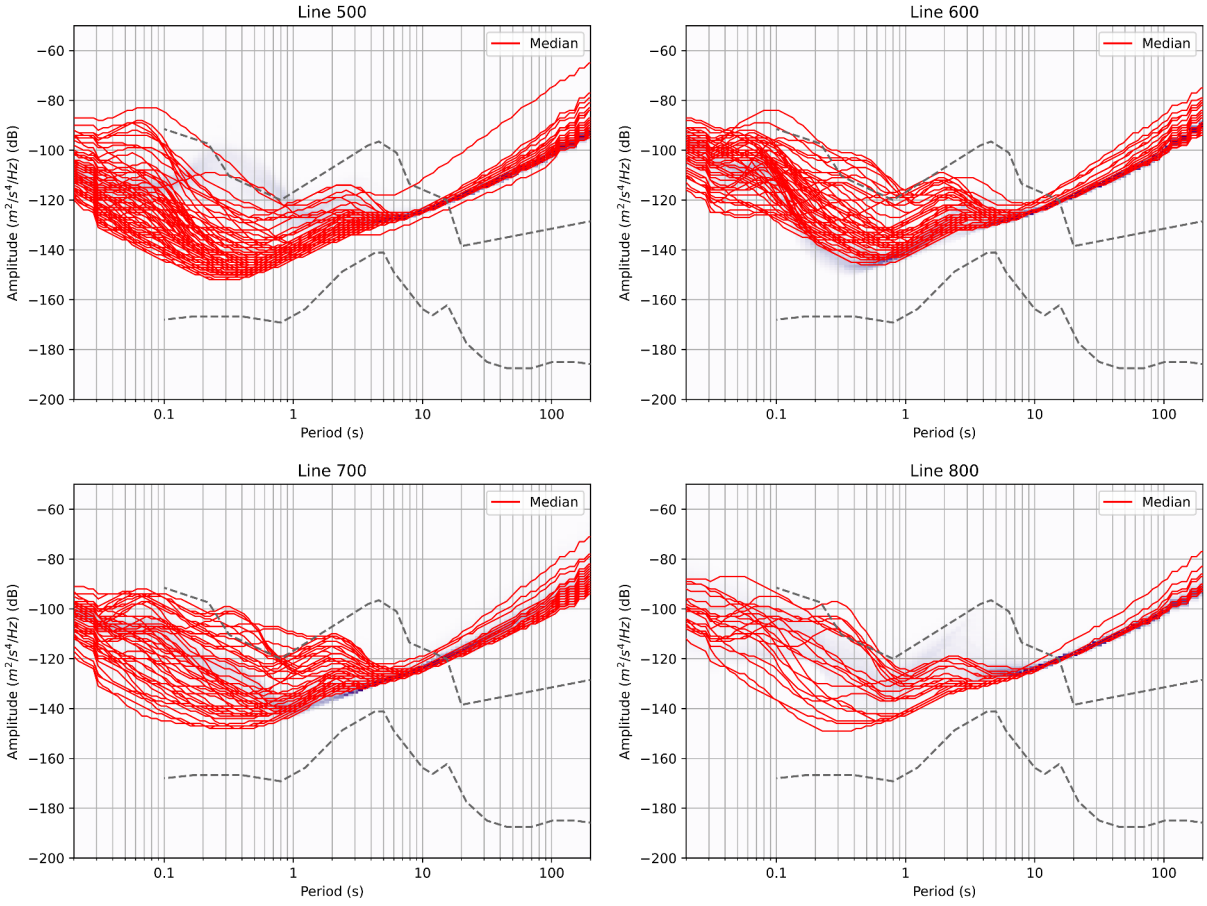

Figure 6. PPSD curves of noise median for short period stations in receiver function lines, corresponding to the second phase of the project.

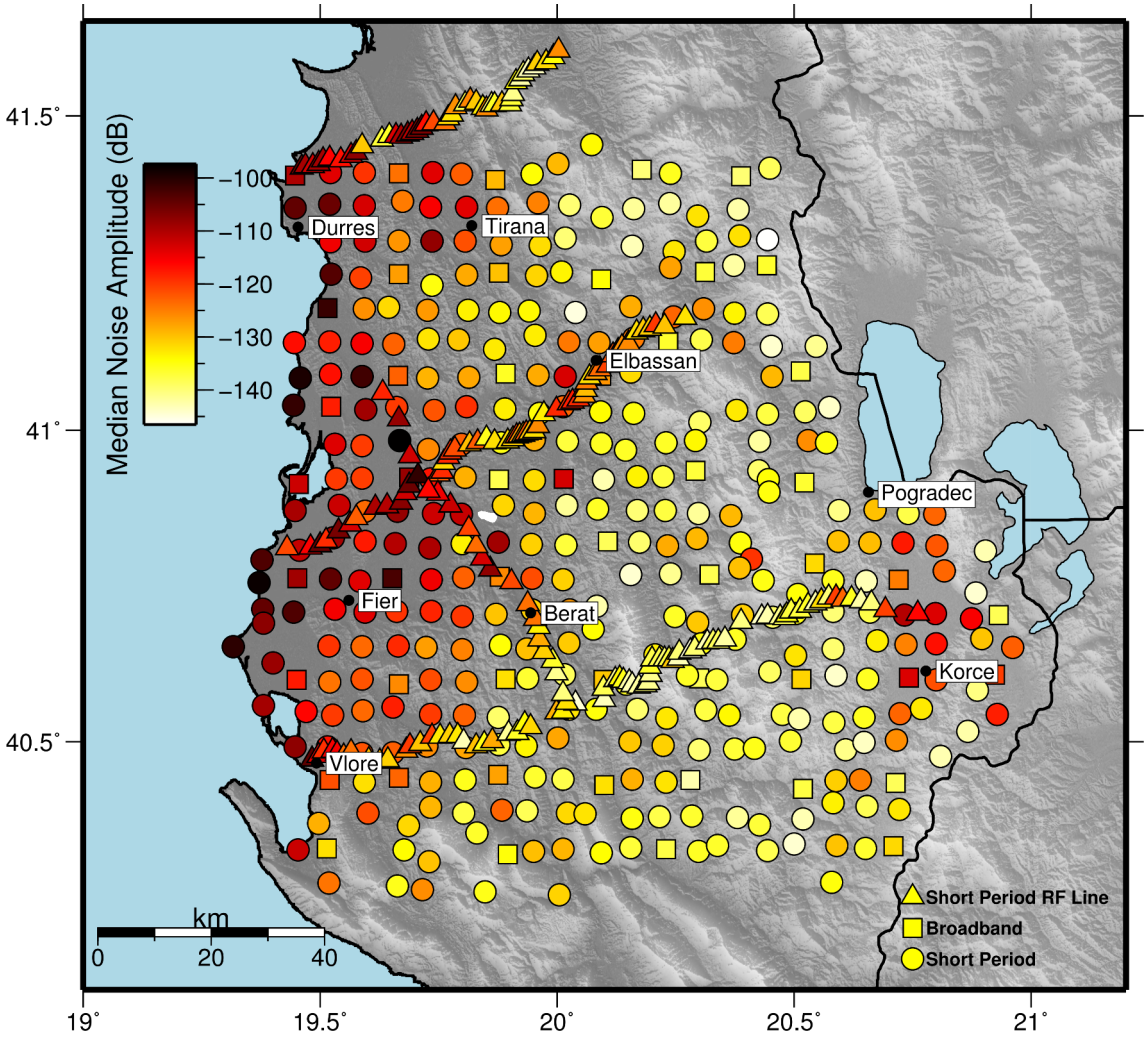

Figure 7. Average of median noise amplitude per station for frequency range 0.05 to 2 s (0.5-20 Hz). Important cities indicated by black dots.

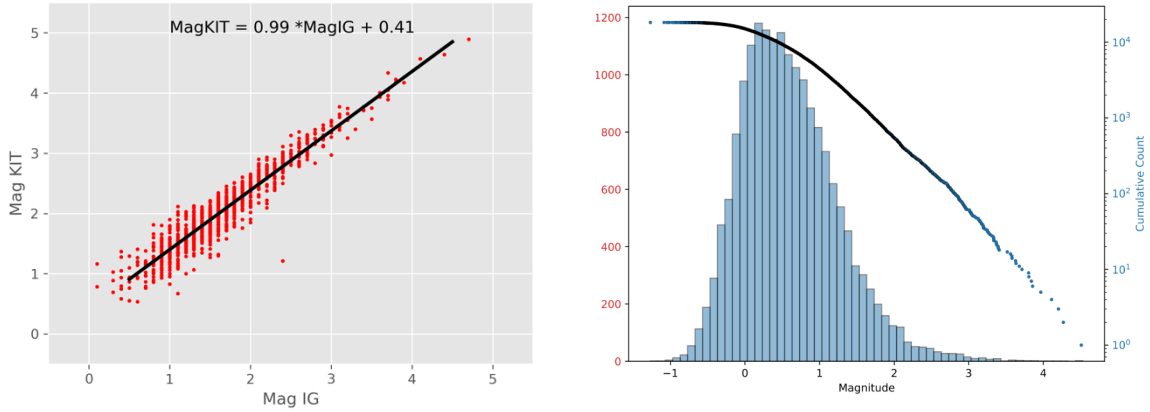

Figure 8. Linear relationship between initial magnitudes from this work and from the IG-PUT local catalogue (left) and frequency-magnitude distribution of final magnitudes (right).

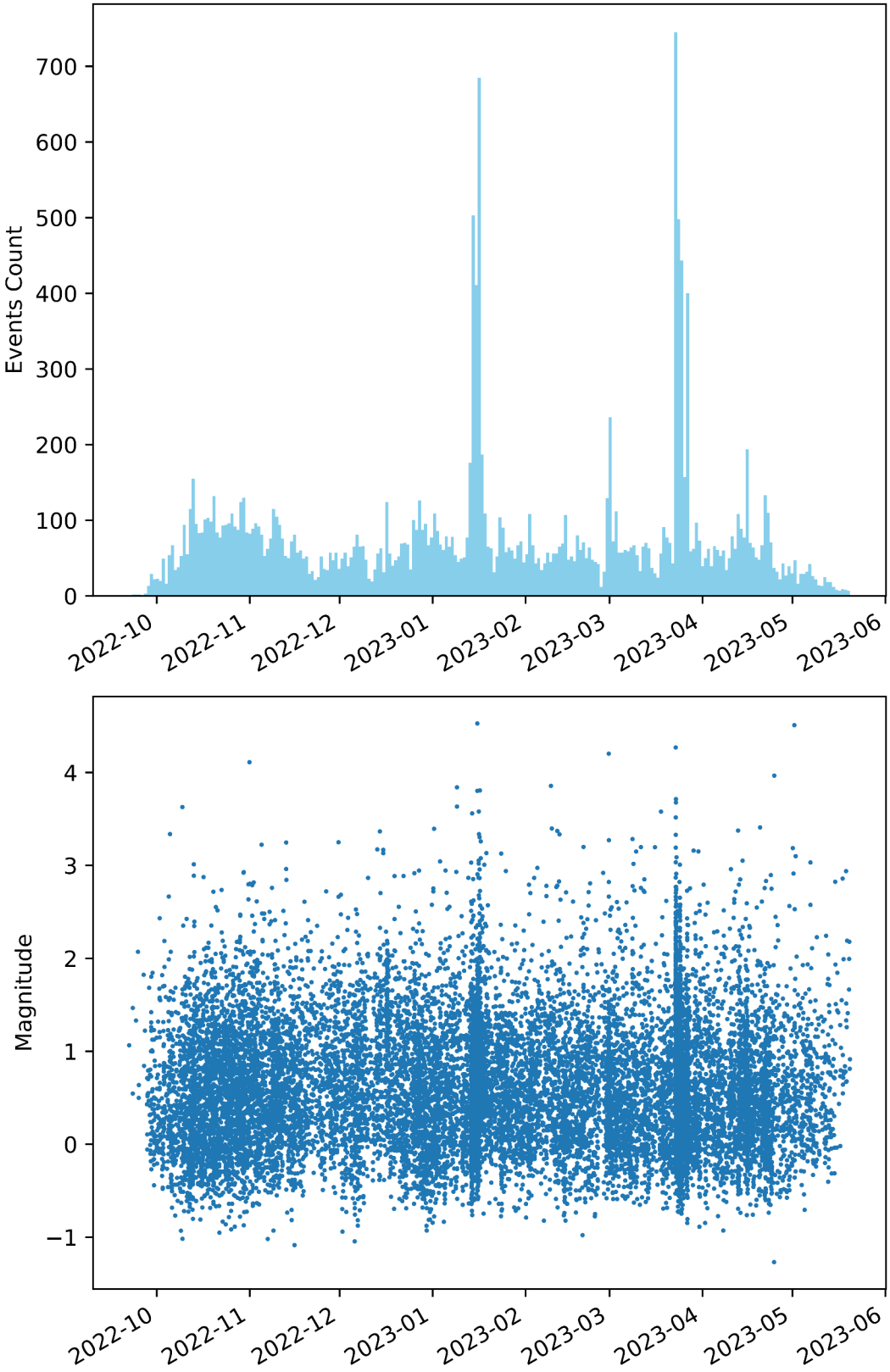

Figure 9. Temporal evolution of seismicity as daily rate (upper panel) and magnitude occurrence (lower panel)

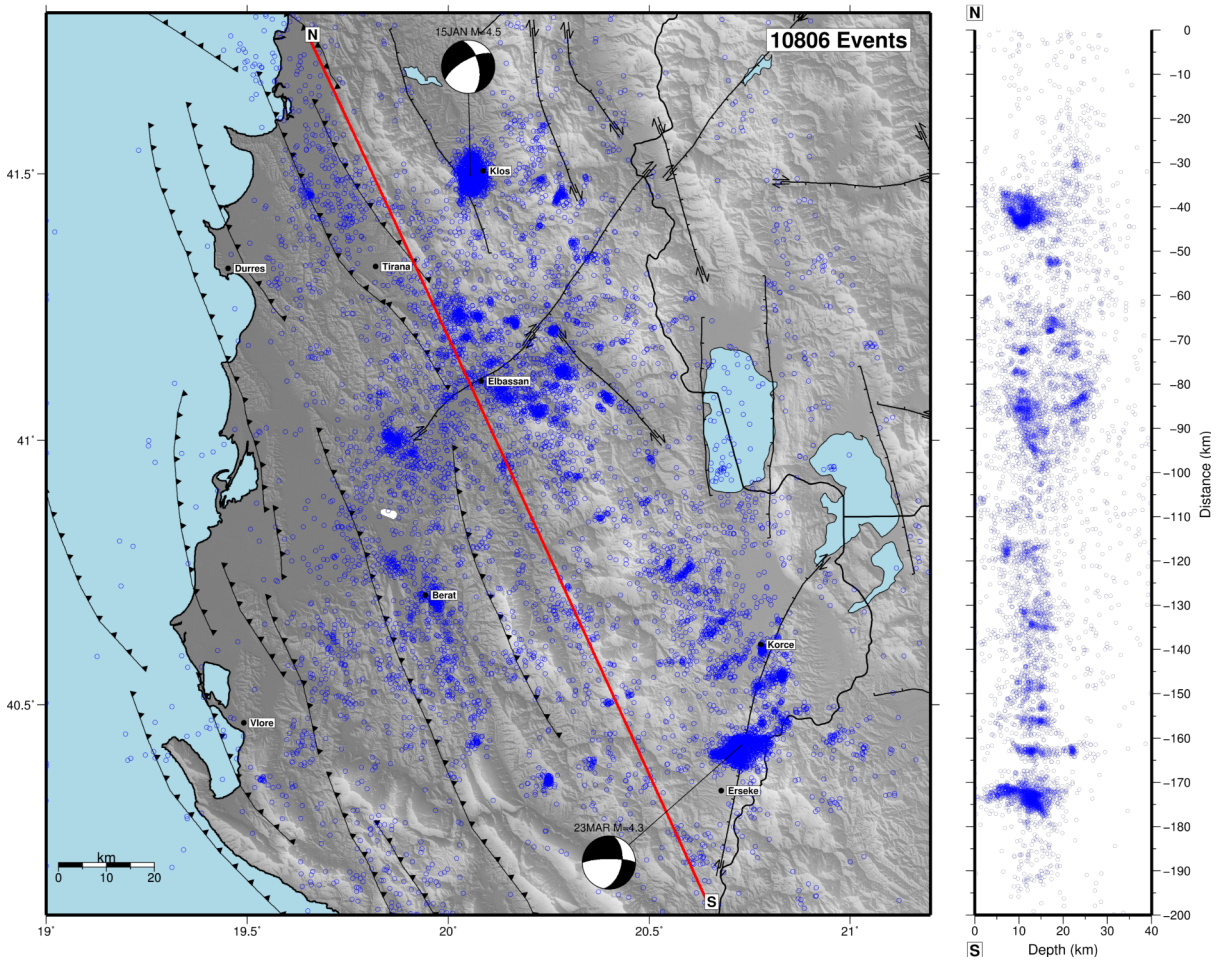

Figure 10. Seismicity map and NW-SE depth section.

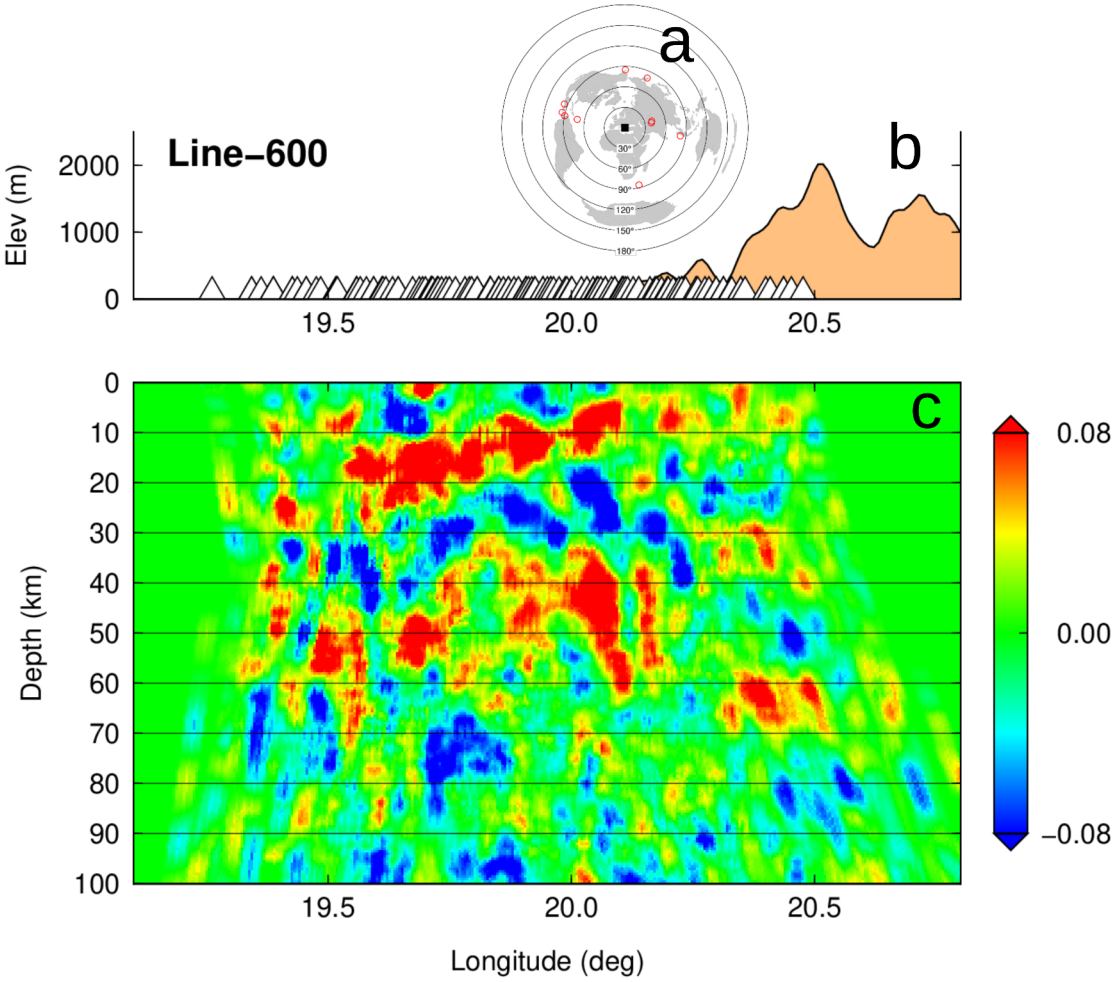

Figure 11. a) Distribution of used teleseismic events (10); b) Elevation profile and stations along Line-600; c) Preliminary RF cross section showing some prominent crustal converters. Red/blue colors indicate positive/negative converted phases, representing downward velocity increase/decrease.

Supplementary Material

The ANTICS Large-N Seismic Deployment in Albania

Hans Agurto-Detzel1*, Andreas Rietbrock1, Frederik Tilmann2,3, Edmond Dushi4, Michael Frietsch1, Ben Heit2, Sofia-Katerina Kufner1,5, Mike Lindner1, Besian Rama4, Bernd Schurr2, Xiaohui Yuan2.

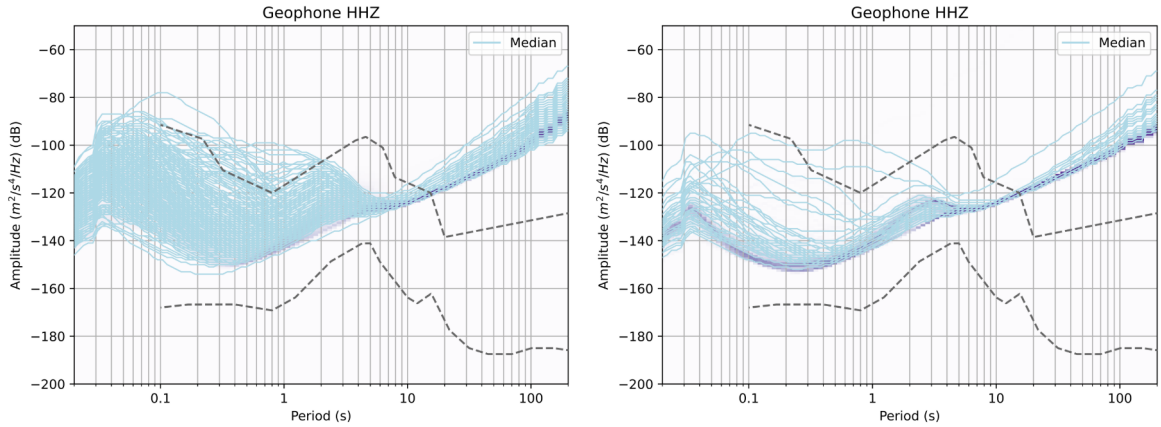

Supplementary Figure 1. PPSD curves of noise median for geophones installed inside properties (left) and outside properties (right).

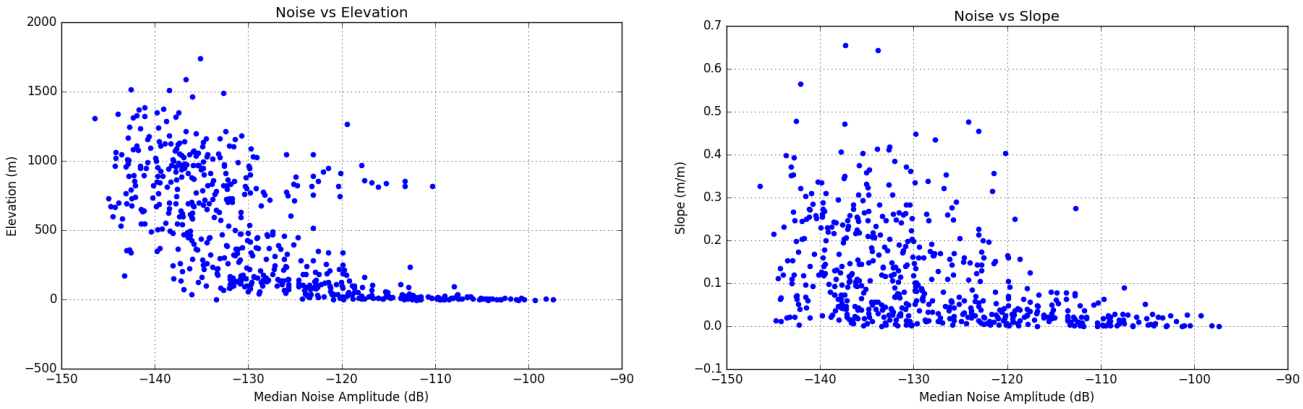

Supplementary Figure 2. Scatter plots of median noise amplitude versus elevation (left) and terrain slope (right) for each site. The slope was calculated as the maximum value from the bidirectional gradient in the SW-NE direction.

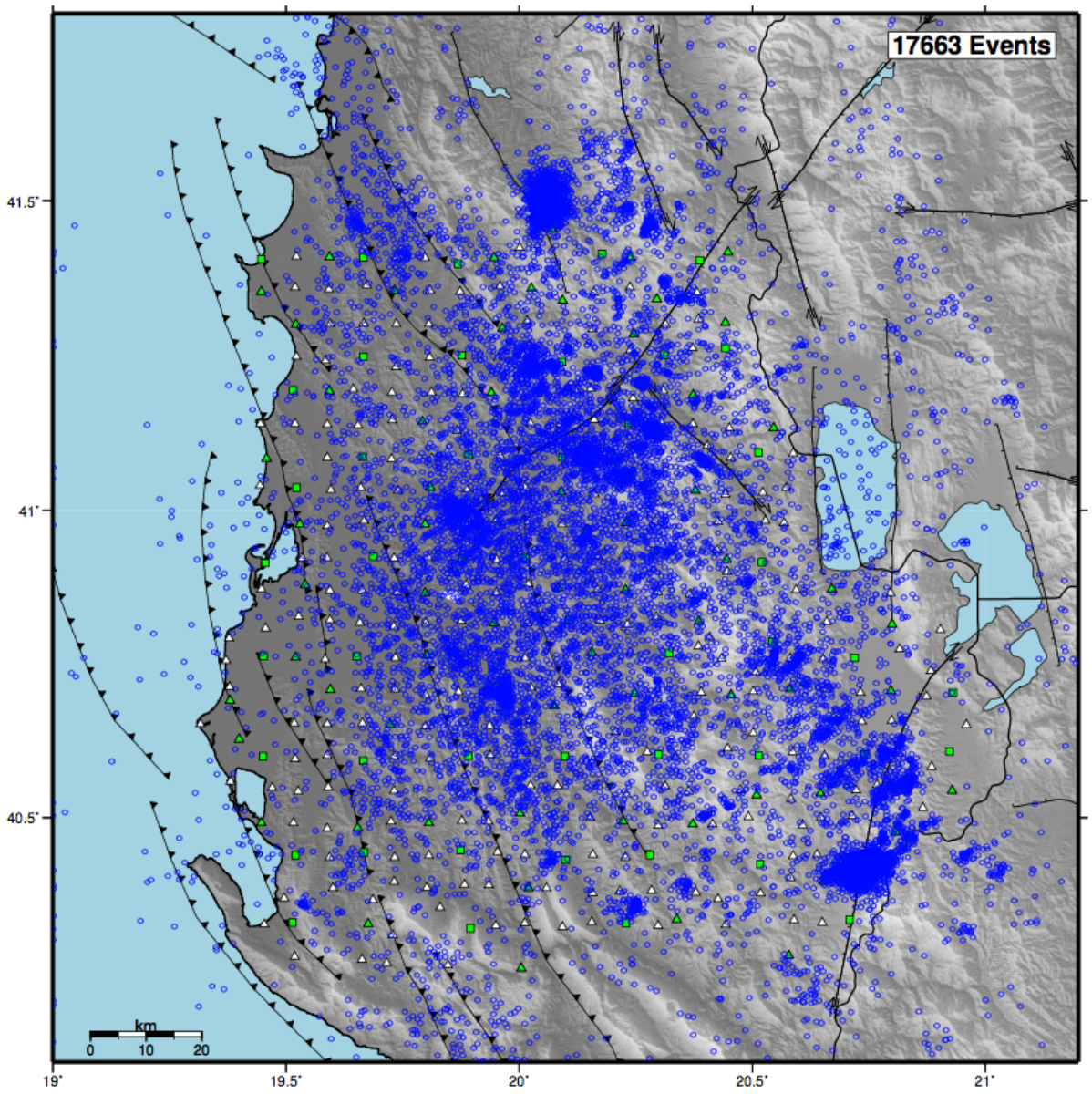

Supplementary Figure 3. Unfiltered complete catalogue with all ~18k events detected. Preliminarily, only stations in green were used for seismicity detection.

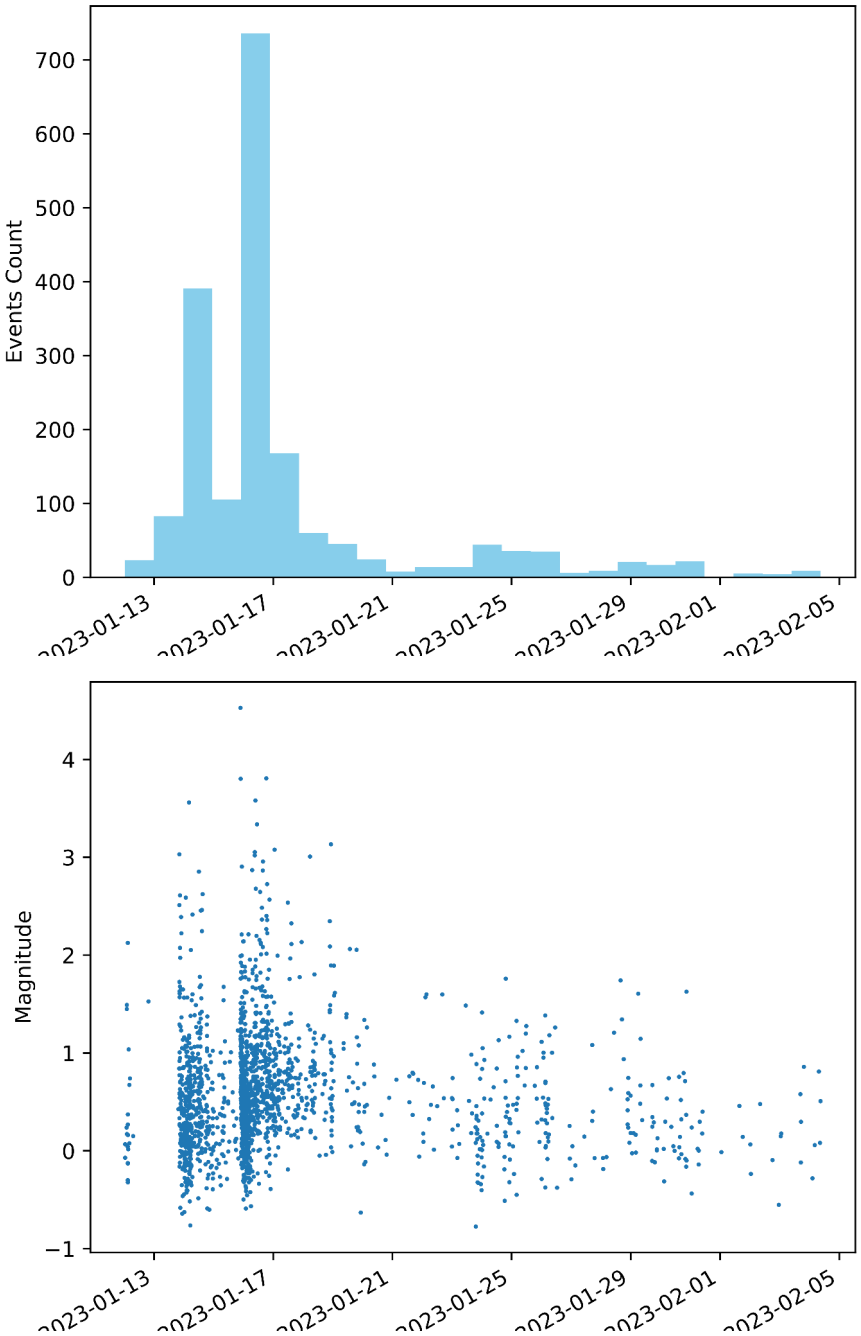

Supplementary Figure 4. Temporal evolution of earthquakes (upper panel) and magnitudes (lower panel) for the Klos sequence during January 2023.

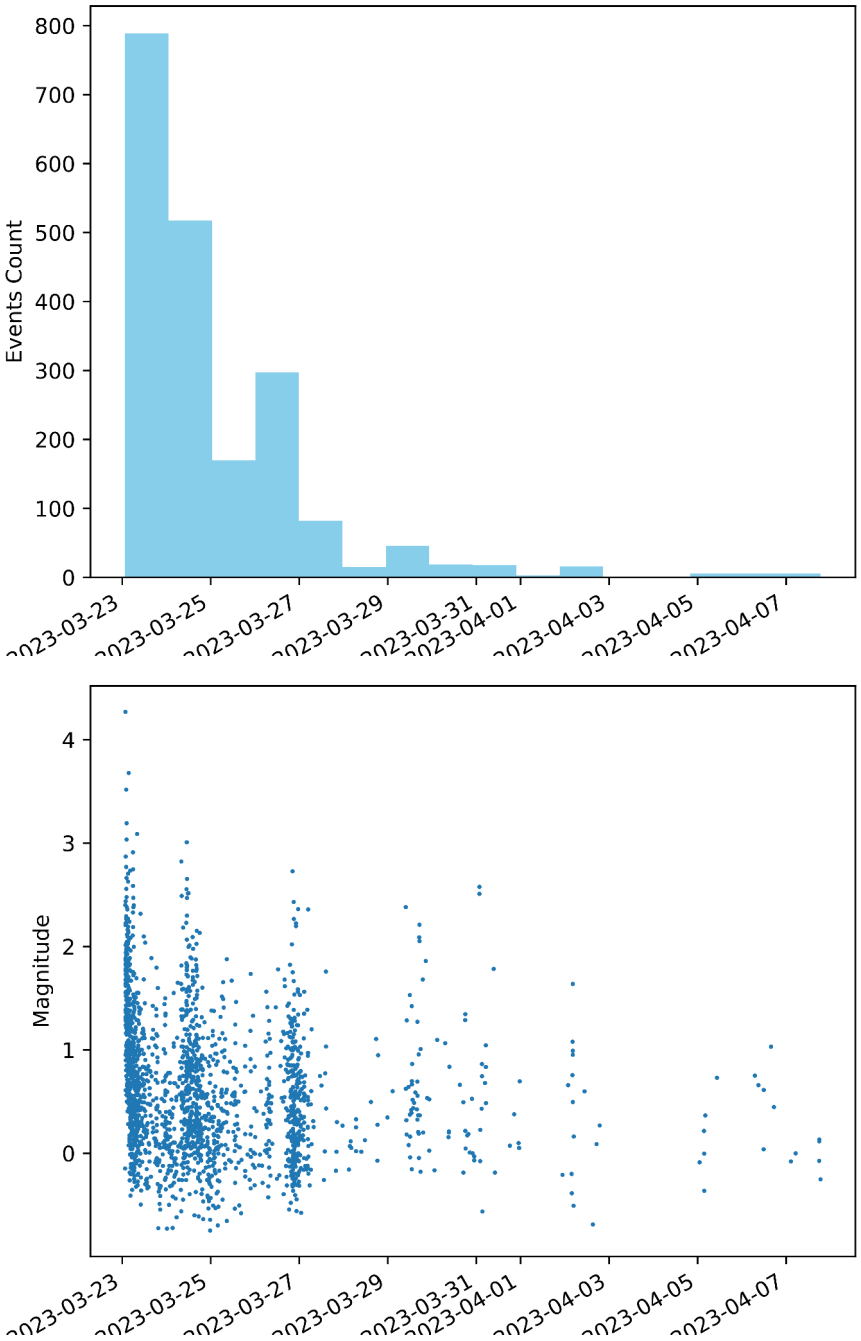

Supplementary Figure 5. Temporal evolution of earthquakes (upper panel) and magnitudes (lower panel) for the Erseke sequence during March 2023.